

Charged Wire Interferometer for Atoms

S. Nowak, N. Stuhler, T. Pfau, and J. Mlynek

Fakultät für Physik, Universität Konstanz, Postfach 5560, D-78457 Konstanz, Germany

(Received 13 May 1998)

We have realized a new type of atom interferometer based on the refraction of matter waves in the radially symmetric electric field of a charged wire. The fringe period shows a power law dependence on the field strength and the de Broglie wavelength. Since the latter dependence is weak, the interferometer has an almost “white light” character. [S0031-9007(98)08090-9]

PACS numbers: 42.50.Vk, 05.30.Jp, 32.80.Pj, 41.20.Cv

Atom interferometers have been successfully applied for precision measurements and the realization of basic gedanken experiments [1]. They consist of three or more atom optical elements to split, redirect, and recombine the motional state of the atoms. These elements are implemented either by freestanding microstructures or by light fields. For high precision applications, such as gyroscopes [2–5], a large throughput of the initial atomic flux is advantageous [6]. In order to efficiently use all atoms in an uncollimated thermal atomic beam, the ideal atom interferometer should produce equally spaced fringes for a wide range of transverse and longitudinal velocities. So called “white light” interferometers solve the problem for different longitudinal velocities by the recombination of only two velocity independent transverse momentum states at the output of the interferometer. Examples for this are the three-grating interferometer [7], operating with a transversely collimated beam, and the Raman interferometer [8]. Operation using a transversely uncollimated atomic beam can also be realized by the Raman interferometer and, for interferometers that do not require light, by the Talbot-Lau interferometer [9]. The latter, in contrast to Ref. [7], operates with three gratings in the Fresnel regime of matter wave diffraction. Since, in this case, many different momentum components build up the interference pattern, the typical length scale of the setup, the Talbot length, depends on the atomic velocity. The Talbot-Lau interferometer is, therefore, chromatic.

In this work, we study a charged wire as the central element in an atom interferometer that requires only microstructures, operates in the Fresnel regime, and accepts, therefore, an uncollimated beam of atoms. At the same time, it has essentially white light character over the range of the atomic velocities in our thermal atomic beam. This makes future extensions of our approach based on microstructures potentially as powerful as, for example, the Raman interferometer gyroscope [5]. The attractive interaction between the induced dipole and the charged wire redirects the atomic trajectories to form a simple interferometer with two spatially separated paths. It can, therefore, also be used to measure the recently proposed topological phase shifts for moving electric dipoles [10–13].

Previous experiments study the diffraction of matter waves from an uncharged wire for electrons [14] and neutrons [15]. A Fresnel biprism for electrons has been demonstrated by charging the wire [14]. The interaction of cold atoms with a charged wire was used in deflection experiments [16] as well as in scattering experiments [17].

A schematic view of the experimental setup is shown in Fig. 1. A beam of metastable helium atoms, predominantly (95%) in the 2^3S_1 state, is generated in a dc gas discharge that can be operated either continuously or in pulsed mode. The polarizability of helium atoms in this state was determined to be $\alpha = 4\pi\epsilon_0 \times 45 \text{ \AA}^3$ [18].

After the passage through a $2 \mu\text{m}$ wide entrance slit, the atomic wave packets evolve freely for a distance $L = 1.3 \text{ m}$, where a tungsten wire with $4 \mu\text{m}$ diam is mounted. From here they travel a further 1.3 m downstream before detection.

Our single atom detector is based on the Auger deexcitation of metastable helium whereby electrons are produced when the atoms hit a metallic electrode. These electrons are then imaged by an electrostatic lens system onto a multichannel plate where they are amplified and

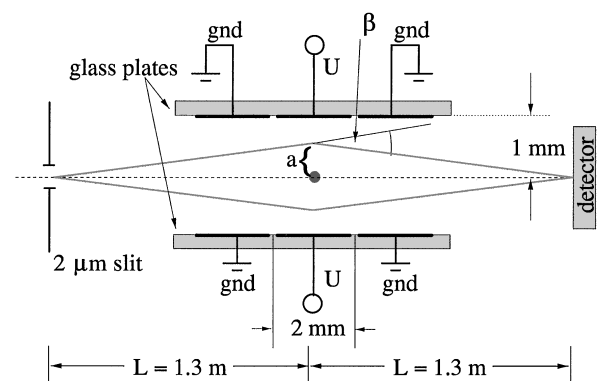


FIG. 1. Schematic view of the experimental setup. The metastable helium beam is produced in a switchable dc gas discharge. The interaction region (drawn not to scale) contains a wire and six planar electrodes. The two middle electrodes were put on the voltage U while the other electrodes and the wire were set on ground potential. The distances between the entrance slit and the wire as well as the distance between the wire and the detector are $L = 1.3 \text{ m}$.

subsequently detected on a resistive area encoder. Since the detector has both time and spatial resolution, the atomic de Broglie waves can be spectrally resolved by the time-of-flight method. This generation and detection scheme for the metastable helium beam has been described in more detail elsewhere [19]. Suffice to say that the width of the atomic velocity distributions amounts to $\Delta v_{(\text{FWHM})}/v = 1/3.8$ for the cw operation and $\Delta v_{(\text{FWHM})}/v = 1/2.5$ in the pulsed mode and that the beam covers the de Broglie wavelength range from 30 to 70 pm with a most probable value of 45 pm for the continuous and for the pulsed mode.

The electrostatic field is generated by setting the wire to ground potential and applying the voltage U to two counterelectrodes. Four guard electrodes are also set to ground potential. This field configuration was chosen to efficiently suppress electric fringe fields.

Initially, a zero electrical field was implemented by setting the wire and the counterelectrodes to ground potential. Figure 2(a) shows the resulting atomic distribution on the detector for a continuously running atomic beam with an integration time of 10 min. The Fresnel fringes due to the diffraction from the wire edges are clearly visible as is the central Poissonian spot which results from the interference of the de Broglie waves originating from the two sides of the wire. The typical count rate on the detector is on the order of 1000 counts/s whereas the background count rate is less than 1 count/s.

In the next step, voltages were symmetrically applied to the two counterelectrodes while the wire was grounded. Figure 2(b) shows several experimental traces all taken for a typical integration time of 10 min. In this configuration it can be seen that as voltage increases the shadow of the wire vanishes and in its place regularly spaced interference fringes appear whose period decreases with increasing voltage.

Let us derive a simple relation to understand the dependence of the fringe period on the applied voltage and

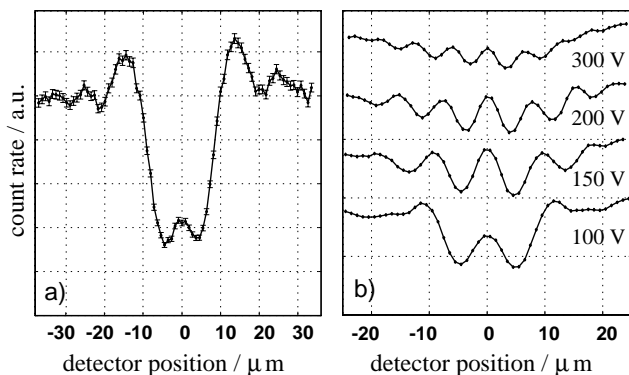


FIG. 2. Measured interference patterns. (a) Uncharged wire: Fresnel fringes and the Poisson spot are visible. The error bars indicate the shot noise level. (b) Different voltages applied to the electrodes: The datasets are plotted with a vertical offset. The dotted horizontal lines indicate the zero level for the respective measurements.

the longitudinal atomic velocity. The spatially dependent potential energy of the atoms in a static electric field $\vec{E}(\vec{r})$ is given by

$$V(\vec{r}) = \frac{1}{2} \alpha |\vec{E}(\vec{r})|^2, \quad (1)$$

where α is the atomic polarizability. The field produced by a charged wire with distant planar electrodes is well approximated near the wire by the field inside a cylindrical capacitor which is given by

$$\vec{E}(r) = U_0 \frac{1}{r} \vec{e}_r. \quad (2)$$

There, $U_0 = U/\ln(r_2/r_1)$, where U is the applied voltage and r_1 and r_2 are the inner and outer radii of a cylindrical capacitor. We verified in numerical calculations that in our case of two distant plane counterelectrodes the field is described in the vicinity of the wire by the same expression where r_2 is then replaced by an effective value of 3 times the distance between the wire and the counterelectrode [20].

In the WKB approximation the phase shift accumulated by the center of mass wave function of an atom moving with velocity v is given by

$$\Delta\phi = \frac{1}{\hbar v} \int_S V(\vec{s}) d\vec{s}. \quad (3)$$

For our experimental parameters, the deviation of the atomic trajectory from a straight line (<10 nm) over the range of the interaction region (<100 μm) is negligible compared to the typical distance from the center of the wire (greater than a few μm), therefore, the charged wire can be treated similar to a thin phase object (Raman-Nath approximation).

The phase shift of an atomic matter wave can then be integrated for a straight trajectory S and is inversely proportional to the distance a to the wire according to

$$\Delta\phi(a) = \frac{1}{4\hbar^2} m \lambda_{\text{dB}} \alpha U_0^2 \frac{1}{a}, \quad (4)$$

where a is the transverse distance of the trajectory from the wire (see Fig. 1). This phase shift gives rise to a small, a dependent deflection of the trajectory by an angle $\beta = -\frac{d\Delta\phi}{da} \frac{\lambda_{\text{dB}}}{2\pi}$ given by

$$\beta(a) = \frac{1}{8\pi\hbar^2} m \lambda_{\text{dB}}^2 \alpha U_0^2 \frac{1}{a^2}. \quad (5)$$

For the interference on the optical axis in the case of the wire placed in the center between a point source and the detector (both distances are L) only trajectories under the angle $\beta(a)/2 = \frac{a}{L}$ originating from the transverse distance

$$a = \pm \sqrt[3]{\frac{L}{16\pi\hbar^2} m \lambda_{\text{dB}}^2 \alpha U_0^2} \quad (6)$$

contribute. The distance a is fixed by the geometry and the interaction parameters, and leads to an expression for the fringe period

$$z_f = \lambda_{dB} \frac{L}{2a} = \frac{\sqrt[3]{\lambda_{dB}}}{\sqrt[3]{U^2 m \alpha}} \sqrt[3]{2\pi L^2 \hbar^2 [\ln(r_2/r_1)]^2} \quad (7)$$

on the optical axis. The same result can be obtained by treating the situation as a scattering problem [21].

z_f is the dominant fringe period in the refraction problem if the diffraction from the edges of the wire can be neglected, which is the case for $z_f \ll 4r_1$, where $4r_1$ is the size of the geometric shadow of the wire on the detector. The other restriction of the model, namely, that the interference pattern is close to the optical axis, implies $z_f \ll a$. Therefore the power law dependence expressed in Eq. (7) should occur for $z_f \ll \sqrt{\lambda_{dB} L}/2$, which for our experimental parameters corresponds to $z_f \ll 6 \mu\text{m}$.

In summary, the fringe period is inversely proportional to $\sqrt[3]{U^2}$ and proportional to $\sqrt[3]{\lambda_{dB}}$. It is this weak dependence on λ_{dB} that gives the almost white light character of the charged wire interferometer and allows for a large number of visible fringes even for thermal atomic beams with a broad velocity distribution. This is in strong contrast to the biprism for electrons [14] where the fringe period is inversely proportional to the applied voltage U and the de Broglie wavelength λ_{dB} .

For comparison with theory, 32 different traces were taken for different voltages and Fourier analyzed. The maximum of the absolute value of the Fourier transformed trace was used to determine the predominant fringe period of the total pattern. Figure 3 shows the result of that measurement in a doubly logarithmic plot. For fringe periods below $8 \mu\text{m}$, z_f decreases with a power law with increasing voltages. The dashed line indicates the prediction by our model without any free parameter and agrees well with respect to the slope, namely, the exponent in the power law and the absolute values for the fringe period within the systematic error in the calibration of the detector. The model breaks down for small voltages as expected when the diffraction from the wire edges becomes important and ultimately dominates the diffraction pattern from the uncharged wire ($U = 0 \text{ V}$).

In a further experiment, we pulsed the atomic beam and measured the diffraction pattern for different de Broglie wavelengths by a time-of-flight technique. The applied voltage was 176 V for which, according to the former measurement, the model can be applied. The result is shown in Fig. 3(b) as a doubly logarithmic plot. Again, the dashed line shows the expectation from our model and agrees well with the measurement. The observed weak dependence of the fringe period on the different de Broglie wavelengths allows us to operate the interferometer with a thermal atomic source, hence, a broad velocity spread. Note that our interferometer operates in the Fresnel regime such as, for example, the chromatic Talbot-Lau interferometer. Replacing the

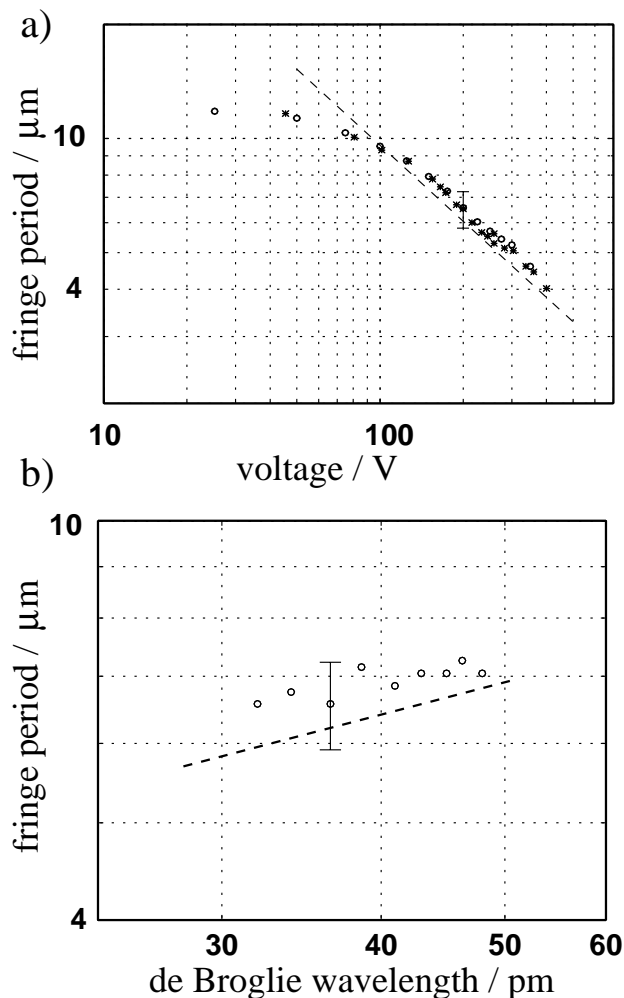


FIG. 3. (a) Measured fringe period for different voltages. Data points indicated by dots and circles refer to two independent experimental runs. The dashed line gives the expected result according to our model without free parameters. The error bar in the experimental result is dominated by the uncertainty in the calibration of the atom detector. (b) Measured fringe period for different de Broglie wavelengths. The dashed line gives the expected result according to our model without free parameters.

single collimation slit with a multiple slit entrance grating [9] (with a period z_f) will, in future experiments, provide a large flux originating from an uncollimated atomic beam. As a result of the large throughput white light interference in combination with an uncollimated atomic beam is the ideal configuration for atom interferometric inertial sensing.

For our actual experiment the calculated resolution of the interferometer with respect to rotations is $0.1 \text{ rad}/\Omega_e$ and the sensitivity amounts to $1.0\Omega_e\sqrt{s}$, where Ω_e is the earth's rotation rate. This is equivalent to the values reported for other arrangements using thermal beams of metastable atoms [3]. If the atomic beam flux of a thermal Cs beam were assumed, the projected resolution would be enhanced by 1 order of magnitude and the sensitivity

by 3 orders of magnitude, which compares well with recently published studies using Cs [5] and Na [4] beams. Compared to the Raman interferometer [5] the advantages of our setup are the simplicity and the lack of internal state dependent systematic phase shifts.

The configuration is also well suited to investigate a new kind of vectorial topological phase for moving electric dipoles that was discussed recently [10–13]. This phase can be thought of as the first term of a Taylor series of topological phases for higher magnetic and electric moments of compound particles. The atom interferometer described in this paper is well suited to measure this topological phase.

In conclusion, we have investigated the diffraction of atomic matter waves from an uncharged and a charged wire. A new, simple, and potentially powerful atom interferometer was demonstrated. The observed power law dependence of the fringe period on the applied voltage and the de Broglie wavelength agrees well with a simple model for the Fresnel diffraction phenomenon. The weak dependence on the de Broglie wavelength and thus the “white light character” of the interference effect give rise to a large number of fringes that are clearly visible even for a thermal source of atoms.

Discussions with U. Leonhardt, K. Rzążewski, J. Audretsch, B. Brezger, A. Peters, and M. Wilkens are acknowledged. This work was supported by the Deutsche Forschungsgemeinschaft.

-
- [1] For an overview on atom interferometry, see *Atom Interferometry*, edited by P. Berman (Academic, San Diego, 1997), and references therein.
 [2] F. Riehle, Th. Kisters, A. Witte, J. Helmcke, and Ch.J. Bordé, *Phys. Rev. Lett.* **67**, 177 (1991).

- [3] M.K. Oberthaler, S. Bernet, E.M. Rasel, J. Schmiedmayer, and A. Zeilinger, *Phys. Rev. A* **54**, 3165 (1996).
 [4] A. Lenef, T.D. Hammond, E.T. Smith, M.S. Chapman, R.A. Rubenstein, and D.E. Pritchard, *Phys. Rev. Lett.* **78**, 760 (1997).
 [5] T.L. Gustavson, P. Bouyer, and M.A. Kasevich, *Phys. Rev. Lett.* **78**, 2046 (1997).
 [6] J.F. Clauser, *Physica (Amsterdam)* **151B**, 262 (1988).
 [7] D.W. Keith, C.R. Ekstrom, Q.A. Turchette, and D.E. Pritchard, *Phys. Rev. Lett.* **66**, 2693 (1991).
 [8] M. Kasevich and S. Chu, *Phys. Rev. Lett.* **67**, 181 (1991).
 [9] J.F. Clauser and S. Li, *Phys. Rev. A* **49**, R2213 (1994).
 [10] M. Wilkens, *Phys. Rev. Lett.* **72**, 5 (1994).
 [11] H. Wei, R. Han, and X. Wei, *Phys. Rev. Lett.* **75**, 2071 (1995).
 [12] J. Audretsch and V.D. Skarzhinsky, *Phys. Lett. A* **241**, 7 (1998).
 [13] U. Leonhardt and M. Wilkens, *Europhys. Lett.* (to be published).
 [14] G. Möllenstedt and H. Düker, *Die Naturwissenschaften* **42**, 41 (1955); G. Möllenstedt and H. Düker, *Z. Phys.* **145**, 377 (1956). In this work electrons interact with a charged wire leading to a deflection angle of their trajectories which is independent of the distance a from the wire. It is therefore often called a biprism for electrons.
 [15] R. Gähler, A.G. Klein, and A. Zeilinger, *Phys. Rev. A* **23**, 1611 (1981).
 [16] F. Shimizu, K. Shimizu, and H. Takuma, *Phys. Rev. A* **46**, R17 (1992).
 [17] J. Denschlag, G. Umshaus, and J. Schmiedmayer, *Phys. Rev. Lett.* **81**, 737 (1998).
 [18] D.A. Crosby and J.C. Zorn, *Phys. Rev. A* **16**, 488 (1977).
 [19] Ch. Kurtsiefer and J. Mlynek, *Appl. Phys. B* **64**, 85 (1996).
 [20] The field configuration in our experimental setup (see Fig. 1) was calculated using a finite element simulation program (MAFIA, version 4.01).
 [21] U. Leonhardt (private communication).